AJNR

Advances in Neuroimaging: Summary of the 26th Annual Meeting of the American Society of N euroradiology, Chicago, May 15–20, 1988

Anne G. Osborn, Barry D. Pressman, William P. Dillon, Van V. Halbach, Robert R. Lukin, A. M. O'Gorman, M. Judith Donovan Post, Val Runge and Douglas H. Yock, Jr.

AJNR Am J Neuroradiol 1988, 9 (5) 985-994
http://www.ajnr.org/content/9/5/985.citation

ASNR Section

Advances in Neuroimaging: Summary of the 26th Annual Meeting of the American Society of Neuroradiology, Chicago, May 15–20, 1988

Anne G. Osborn,[1] Barry D. Pressman,[2] William P. Dillon,[3] Van V. Halbach,[3] Robert R. Lukin,[4] A. M. O'Gorman,[5] M. Judith Donovan Post,[6] Val Runge,[7] and Douglas H. Yock, Jr.[8]

The 26th annual meeting of the American Society of Neuroradiology (ASNR) was held in Chicago, May 15–20, 1988. The meeting began with its first-ever categorical course, Spine and Cord Imaging, and continued with scientific sessions on a variety of topics ranging from new techniques in MR to advances in surgical neuroangiography. More than 200 oral presentations, 60 scientific exhibits, and a large technical exhibit section were featured.

The following meeting highlights summarize a selection of the most up-to-date information available in neuroradiology as presented at this year's ASNR. First authors of the presentations cited are listed in parentheses or brackets. Full abstracts start on page 1001 of this issue of the *American Journal of Neuroradiology.*

Brain

Clinical

Papers presented in the various sessions focusing on brain imaging emphasized MR imaging and reflected several trends: (1) increasing clinical experience with specific diseases, (2) better understanding of normal variants and technical artifacts, and (3) further studies of the mechanisms underlying alterations in signal intensity.

Clinical experience with MR has led to increasing recognition of characteristic patterns for many diseases. For example, it was reported that primary cerebral lymphoma often appears nearly isointense on T1- and T2-weighted images (Shapiro; Olsen). Adenocarcinoma metastatic to the brain frequently has relatively low signal intensity on T2-weighted images (Hinshaw). Ependymomas of the fourth ventricle may be distinguishable from medulloblastomas because the former tend to contain more peripheral cysts and are more heterogeneous. In addition, ependymomas more commonly extend caudally through the vallecula and foramen magnum and have generally higher signal intensity on T2-weighted images (Bury). Relatively isointense signal from pituitary macroadenoma on T2-weighted images often is associated with a firm or fibrous texture at surgery (Johnson). Prominent high signal intensity on T2-weighted images from a temporal lobe lesion in a patient with seizures suggests neoplasm, as opposed to the more modest signal increase seen frequently in mesial temporal sclerosis (Heinz).

[1] University Medical Center, Salt Lake City, UT 83132. Address reprint requests to A. G. Osborn.
[2] Cedars Sinai Medical Center, Los Angeles, CA 90048.
[3] University of California, San Francisco, San Francisco, CA 94143.
[4] University Hospital, Cincinnati, OH 45267.
[5] Montreal Children's Hospital, Montreal, Quebec, Canada H3H 1P3.
[6] University of Miami School of Medicine, Miami, FL 33101.
[7] New England Medical Center Hospital, Boston, MA 02111.
[8] Abbott Northwestern Hospital, Minneapolis, MN 55407.

AJNR 9:985–994, September/October 1988 0195–6108/88/0905–0985

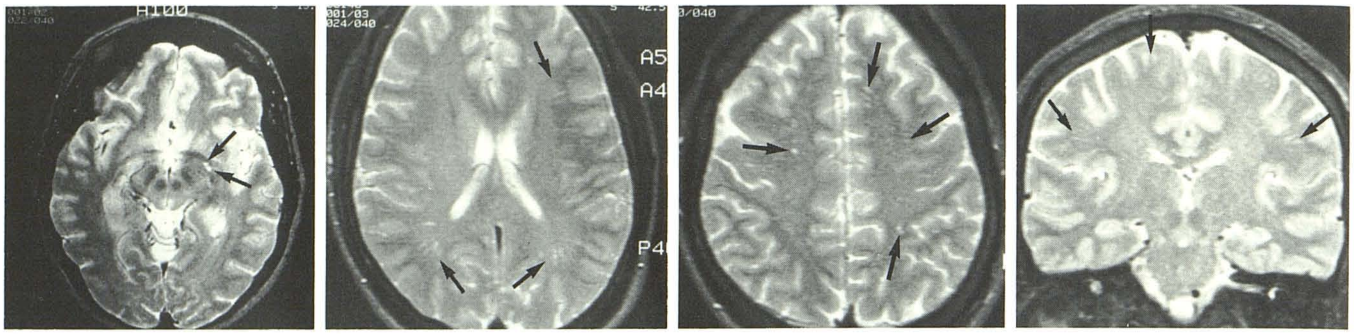

A B C D

Fig. 1.—T2-weighted MR images show prominent but normal perivascular spaces in a 55-year-old woman.

***A*, Axial image through basal ganglia shows two prominent asymmetric foci of increased signal. These are large Virchow-Robin spaces along course of lenticulostriate arteries (*arrows*).**

***B*, Axial image at mid-ventricular level shows symmetric linear foci of increased signal in the hemispheric white matter (*arrows*). These fine, linear rays represent dilated perivascular spaces.**

***C*, Axial image through upper part of centrum semiovale shows additional dilated perivascular spaces (*arrows*). These appear somewhat linear in frontal lobes, where they are sectioned parallel to the image plane; more posteriorly they are seen in cross section and appear round.**

***D*, Coronal image shows fine, linear raylike foci of increased signal (*arrows*) extending centripetally from subcortical white matter toward centrum semiovale. (Courtesy of Dr. Boyko)**

At the same time, additional experience with MR has shown overlapping appearances for many other lesions. For example, a cerebral mass with relatively low signal intensity on T2-weighted images could represent hemosiderin-containing hemorrhagic metastasis, iron-containing chloroma, occult vascular malformation, and so on.

Ependymitis can cause signal changes and thickening of the corpus callosum that resemble involvement by a primary glioma (Kochan). Patients with chronic hepatic failure may have central high-signal lesions within the pons on T2-weighted images that are indistinguishable from classic central pontine myelinolysis (Brunberg).

On cerebral MR, better understanding of anatomic variants, the appearance of the aging brain, and technical artifacts allow these entities to be distinguished from pathologic changes. Several papers (Heier; Muraki; Boyko) reported that large Virchow-Robin spaces can accompany penetrating arteries deep into cerebral parenchyma. These long, thin perivascular spaces have a linear or curvilinear pattern entering the basal ganglia (along the course of the lenticulostriate arteries) from the anterior perforated substance near the base of the brain (Fig. 1A) or radiating centripetally into hemispheric white matter from the cortical surface more superiorly (Figs. 1B–1D). On high-quality T2-weighted images, these perivascular spaces are commonly seen as fine "rays" when parallel to the scan plane (e.g., near the anterior commissure at the base of the brain and over the vertex on axial scans). There appears to be congenital variation in the size of the perivascular spaces and a general tendency to become increasingly prominent with age. Their uniform small diameter, frequent symmetry, and characteristic locations allow distinction from white-matter infarcts or demyelinating disease.

The smooth, uniform layer of high signal intensity seen immediately adjacent to ventricular margins on long TR images in many elderly patients appears to represent both structural and functional phenomena (Heier). A zone of "myelin pallor" is found at autopsy in this region (Fig. 2), but the paraventricular high-signal layer on MR probably also reflects accumulation of fluid on its way from the white matter to the ventricles. This finding correlates with age, hypertension, and white-matter disease, and it may be a secondary manifestation of "leaky" white matter in these circumstances that cause increased circulation of interstitial fluid. The regularity and subependymal location of this MR finding distinguish it from the patchy configuration and white-matter location of most infarcts and demyelinating plaques.

At high field strengths, chemical-shift artifacts can create the false impression of a small subdural collection (along the frequency-encoding axis) (Smith). This artifactual appearance can be several millimeters thick at 1.5 T (Fig. 3) and is accentuated by a narrow band width or large fields of view. It is most prominent at relatively short TEs and is less disturbing on heavily T2-weighted images. The artifact tapers symmetrically at its margins (i.e., anteriorly and posteriorly if

2

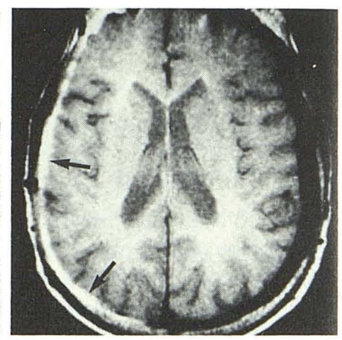

3

Fig. 2.—Photomicrograph shows lateral ventricle (seen as empty space at upper left-hand corner) and adjacent subependymal structures stained with Luxol Fast Blue for myelin. A = arteriosclerosis; P = myelin pallor (width); E = ependymal denudation; R = rosette. (Courtesy of Dr. Heier)

Fig. 3.—Axial T1-weighted MR image with chemical shift artifact shows pseudo subdural hematoma (*arrows*). (Courtesy of Dr. Lanzieri)

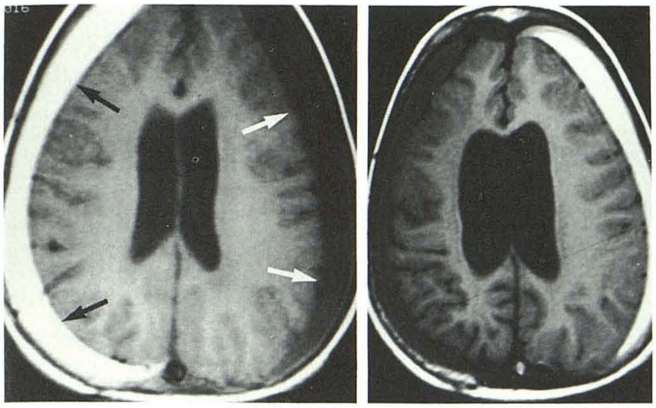

A B

Fig. 4.—*A*, T1-weighted axial MR image shows high signal of right-sided subacute subdural hematoma (SDH) (*black arrows*) and acute recurrent left-sided SDH (*white arrows*) with low-signal extraaxial collection.

B, T1-weighted axial image obtained 4 months later shows evolution of right-sided SDH from high-intensity, subacute to low-intensity, chronic SDH. Left-sided lesion has evolved from acute to subacute. (Courtesy of Dr. Fobben)

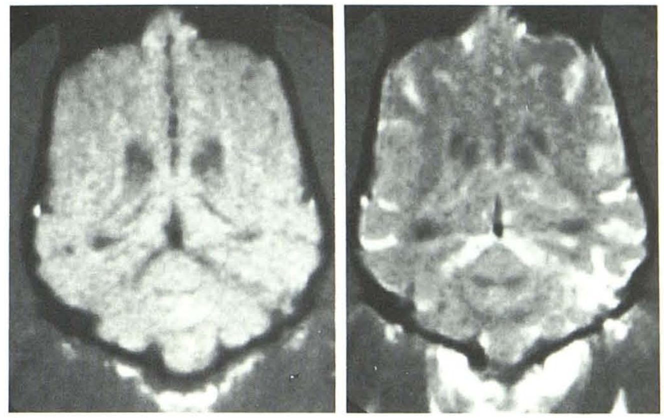

A B

Fig. 5.—*A* and *B*, MR images of the brain before (*A*) and after (*B*) IV injection of Gd-DTPA in a canine model of meningitis show enhancement of meninges after administration of gadolinium, paralleling extent of disease as shown pathologically. (Courtesy of Dr. Mathews)

the frequency axis is right/left on an axial image), unlike many real subdural hematomas.

True subdural collections can present a spectrum of MR appearances (Fig. 4) (Fobben). Blood elements go through the same general series of intensity changes described for intracerebral hemorrhage. However, methemoglobin in subdural hematomas seems to disappear rapidly; the presence of persistent T1 shortening suggests rehemorrhaging. Similarly, hemosiderin is rarely noted in subdural hematomas unless hemorrhages are recurrent. Organization of chronic subdural hematomas can produce a picture of "meningeal fibrosis" (Destian) with dense subdural enhancement on CT scans that is seen to be adjacent to (but distinct from) the dural structures seen on MR images. Subdural hygromas do not have the evolving signal of blood products seen in hemorrhages; however, the signal intensity of fluid within a hygroma is often higher than that of CSF elsewhere, possibly because of loculation reducing pulsation and spin dephasing.

William R. Shapiro, Chairman of Neurology at Memorial Sloan Kettering Cancer Center, reviewed recent laboratory and clinical investigation in primary brain tumors. He noted that the one- or two-log reduction in tumor-cell burden accomplished by subtotal or "complete" resection correlates with improved survival after radiation and/or chemotherapy, supporting an aggressive surgical approach to accessible masses (as opposed to stereotactic biopsy).

The Dyke Award paper (Mathews) described prominent gadolinium enhancement on MR images of dogs with experimentally induced bacterial meningitis (Fig. 5). Enhancement of the meninges seems to be considerably more sensitive on MR than on contrast-enhanced CT, partially because of the absence of calvarial artifacts on MR and its multiplanar display. Meningeal enhancement on MR has also been noted in neoplastic and acute and chronic inflammatory conditions (Fig. 6) (Kanal; Blaser).

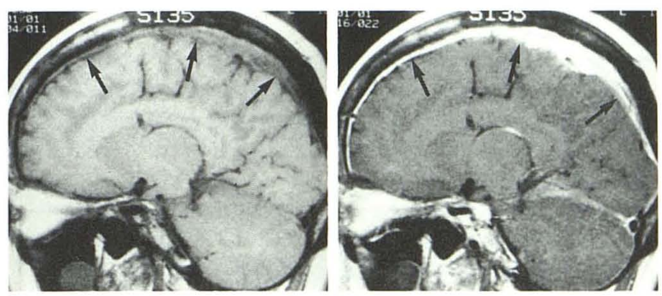

A B

Fig. 6.—*A* and *B*, Sagittal T1-weighted MR images before (*A*) and after (*B*) IV infusion of Gd-DTPA show marked meningeal enhancement (*arrows*) in a patient with aseptic meningitis. (Courtesy of Dr. Kanal)

Despite the increased sensitivity of MR compared with CT for most categories of cerebral disease, it is clear that MR is not infallible. Essentially isointense lesions continue to be reported (e.g., some fibrillary astrocytomas) (Lee). More important, examples of normal MR images in the setting of proved pathologic changes are many, including mesial temporal sclerosis (Lee; Heinz) and mild ischemic changes (DeLaPaz). That is, there seems to be an as yet poorly defined threshold for MR detection in many cerebral diseases.

Another reason for continued humility among MR interpreters is the increasingly complex nature of observations in specific pathologic changes, notably, intracranial hemorrhage. The multifaceted progression of signal changes previously described in intracerebral hematomas and correlated with specific hemoglobin products may be only part of the picture. Thrombus within aneurysms (Brothers) or in extracerebral collections (Fobben) behaves differently and, at this point, less predictably. Gradient echoes detect prominent magnetic

7A 7B

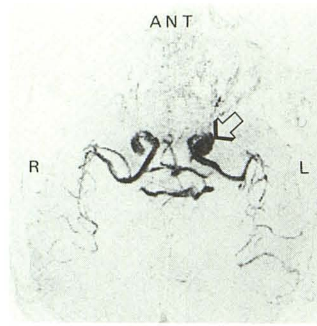

8

Fig. 7.—*A* and *B*, 1-mm reformatted axial (*A*) and coronal (*B*) MR images obtained by contrast-enhanced three-dimensional FLASH examination in a patient with a planum sphenoidale meningioma. From a single T1 acquisition, high-resolution T1-weighted images can be reformatted in any desired plane. (Courtesy of Dr. Runge)

Fig. 8.—MR angiogram shows juxtasellar aneurysm (*arrow*) originating from anterior loop of carotid siphon as seen in submental vertex projection. (Courtesy of Dr. Masaryk)

susceptibility changes almost immediately in experimental acute intracerebral hematomas (Weingarten), not correlating with the anticipated evolution of deoxyhemoglobin (and therefore suggesting a role for gradient-echo techniques in the early diagnosis of intracerebral hemorrhage).

Efforts to elucidate and exploit the effects of CSF motion on cerebral MR images continue. Examples include the explanation of prominent intraventricular signal loss under conditions of aqueductal dilatation (due to increased pulsation amplitude allowed by reduced aqueductal resistance) (Whittemore). A related example is the attempt to base prognosis and shunt response in syringomyelia on the degree of cyst pulsation (Post). CSF "flow maps" with cranial and spinal applications are also possible when gradient-echo techniques are used (Rubin).

Continuing evidence for the superiority of MR imaging in the detection of intracranial disease was presented in the study titled "A Prospective Study of MR in Posterior Circulation Infarction" from Melbourne, Australia. In 44% of cases, the MR examination was positive for infarction in the posterior circulation despite negative findings on CT examination.

Scientifically rigorous prospective studies on the comparative clinical efficacy of MR and other innovative imaging techniques and qualitative or descriptive reports are needed in our rapidly changing subspecialty. In addition to the specific advances in cerebral MR discussed during the meeting, several general perspectives were raised. One was the clear recognition that MR, although offering excellent demonstration of structure, is currently limited in its ability to assess function. For example, determination of residual/recurrent tumor appears to be better accomplished by single-photon emission CT (SPECT) scanning with thallium-201 than by MR (Boyko). More generally, the next advances in neuroimaging most likely will occur through functional mapping, such as neurotransmitter and receptor analysis, based on SPECT and positron emission tomography.

Technical

A number of technological innovations were introduced for MR imaging. These included the use of three-dimensional (3D) fast low-angle shot imaging (FLASH) for examination of the cervical spine (Hueftle) and brain (Runge) (Fig. 7). The

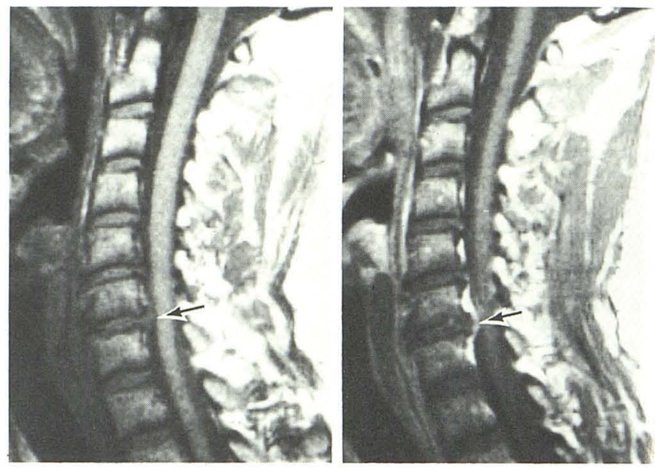

A B

Fig. 9.—*A* and *B*, MR images of cervical disk herniation (nonoperated spine) before (*A*) and after (*B*) injection of Gd-DTPA show increased conspicuity of a disk (*arrows*) at C6–C7 level after enhancement of epidural venous plexus. (Courtesy of Dr. Modic)

technique allows for rapid, high-resolution, multiplanar, reformatted studies.

Some exciting work was presented on MR angiography and the depiction of CSF flow. The use of combined rephased and dephased sequences for MR angiography has allowed exquisite images of the carotid bifurcation (Wagle) and intracranial circulation (Masaryk). Further refinements of these techniques may result in a reliable noninvasive test for the diagnosis of vascular disease (Fig. 8). Other authors (Kucharczyk) indicated that if fast field-echo techniques were used, dynamic and static fluids could be reliably differentiated. This simple and rapid technique may allow improved study of CSF dynamics.

Spine and Spinal Cord

Clinical

Two studies (Quencer; Post) elucidated the usefulness of MR in evaluating acute traumatic injuries of the spinal cord. With the introduction of nonferromagnetic traction devices,

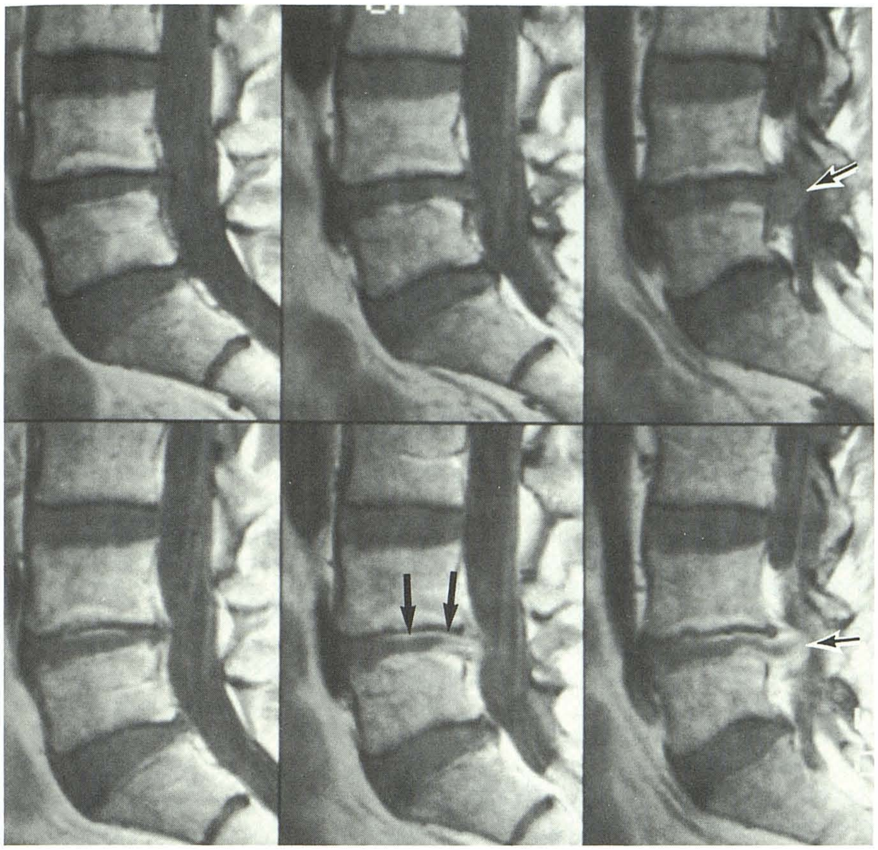

Fig. 10.—3-mm sagittal, adjacent T1-weighted (500/17) spin-echo MR images before (*top*) and after (*bottom*) administration of Gd-DTPA show postoperative scar and recurrent disk herniation. Soft-tissue mass (*black-and-white arrows*) extending posteriorly at L4–L5 interspace shows peripheral enhancement after administration of gadolinium. Note linear area of enhancement along superior margin of disk margin (*black arrows*). (Courtesy of Dr. Modic)

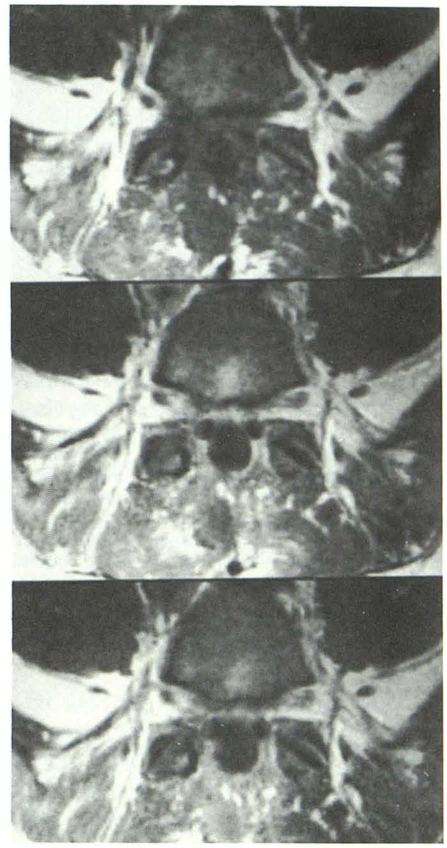

Fig. 11.—Axial T1-weighted (500/17) MR images before and after administration of Gd-DTPA show scar only from disk herniation. Images before administration of gadolinium show a soft-tissue signal intensity surrounding thecal sac and no descernible nerve roots. Images after administration show enhancement surrounding thecal sac and better definition of nerve roots. No non-enhancing structure that would suggest disk herniation is seen. (Courtesy of Dr. Modic)

this is now technically feasible. In the acute setting, MR may be useful when a patient's clinical status suddenly deteriorates or when findings on clinical examination do not agree with those on X-ray CT. Epidural hematomas and traumatic disk herniation are probably best recognized on MR. For evaluation of long-term traumatic sequelae, the pulsatile characteristic of posttraumatic spinal cord cysts can be recognized by using cine MR techniques. This may have prognostic significance, as the suggestion was made that large pulsatile cysts are associated with progressive neurologic symptoms (Post).

Herniated thoracic disks were recognized in 2% of lumbar MR studies performed for symptoms of lumbar spine degenerative disease (Tourje). This discovery of a relatively high percentage of thoracic disk herniations is even more remarkable inasmuch as the field of view routinely included only T10 and below in this study. Thoracic disk herniations had previously been estimated to be less than 0.3% of all disk herniations.

Enhancement of venous plexus and vascular granulation tissue surrounding virgin disk herniation was useful in both the cervical and thoracic spine for better recognition of herniated disks on MR (Fig. 9) (Montanez). MR with Gd-DTPA was also helpful in distinguishing postoperative scars and recurrent disk herniation (Fig. 10) from scar alone (Fig. 11) (Modic). Two papers (Sze; Manelfe) reported the use of Gd-DTPA–enhanced MR in spinal cord lesions. Recognition of lesion nidus, particularly with hemangioblastomas and metastatic disease, was improved. The separation of astrocytoma from surrounding cord edema was highlighted with Gd-DTPA, allowing better direction of biopsy. MR with Gd-DTPA enhancement distinguished solid from cystic components in neoplastic disease.

A correlative pathologic study illustrated that the intranuclear cleft, visualized as a dark line in the middle of the intervertebral disk on T2-weighted images, was due primarily to collagen (Haughton). This develops with aging from ventral and dorsal aspects of the disk, proceeding toward the center.

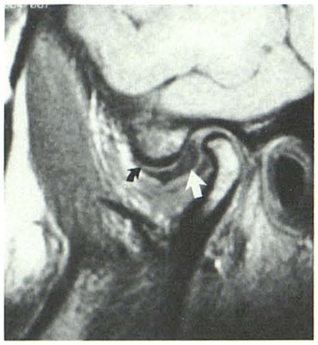

Fig. 12.—Sagittal T1-weighted (600/20) 3-mm-thick, closed-mouth MR image of temporomandibular joint shows anterior displacement of deformed meniscus (*white arrow*) with effusion (*curved black arrow*) in superior joint compartment. Increased meniscus signal represents myxomatous degeneration of fibrocartilage, which was confirmed surgically. (Courtesy of Dr. Schellhas)

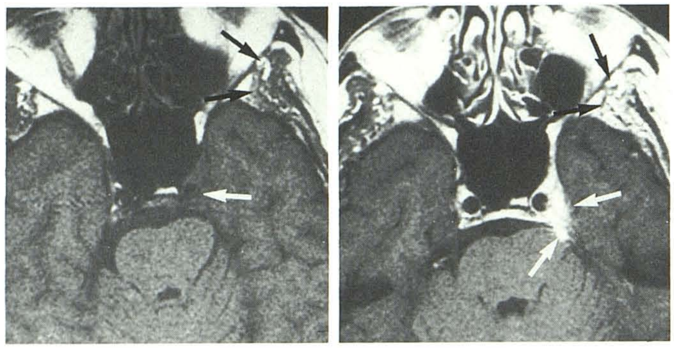

A B

Fig. 13.—Axial T1-weighted MR images in a patient who had trigeminal neuralgia 2 years after resection of a spindle-cell carcinoma of left cheek and orbit show fatty infiltration of left temporalis muscle (*black arrows*), suggesting denervation atrophy of muscles of mastication (supplied by fifth cranial nerve).

***A*, Unenhanced MR image shows slight, questionable enlargement of left side of upper pons and slight asymmetry of cavernous sinus, with questionable abnormal soft tissue (*white arrow*) adjacent to internal carotid artery.**

***B*, Gadolinium-enhanced MR image in same plane shows definite perineural tumor spread along fifth cranial nerve, extending into its root entry zone (*white arrows*). (Courtesy of Dr. Crawford)**

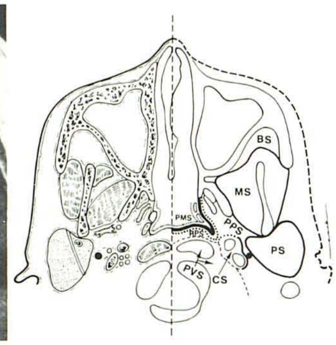

Fig. 14.—Drawing of axial nasopharynx shows three layers of deep cervical fascia and spaces they define. *Heavy solid line* = superficial layer; *dotted line* = middle layer, and *dashed line* = deep layer. PPS = parapharyngeal space, PMS = pharyngeal mucosal space, MS = masticator space, PS = parotid space, CS = carotid space, RPS = retropharyngeal space, PVS = prevertebral space. (Courtesy of Drs. Harnsberger and Dillon)

Technical

The use of low band widths for improved signal-to-noise imaging of the spine was presented (Ketonen). Low band widths decrease random noise in the image, improving the overall signal-to-noise ratio, although they do increase chemical-shift artifacts. Experience with gradient-echo techniques continues to accumulate. Two studies indicated that T1- and T2-weighted spin-echo images were, for the most part, superior to gradient-echo images in the diagnosis of lumbar disk disease (Gusnard; Citrin). However, the use of gradient-echo techniques for the diagnosis of cervical disk disease continues to be advocated. Results with STIR (short T1 inversion recovery) showed potential for improved detection of neurofibromas, intraspinal lesions, and bony metastases (Schnapf). With STIR, the fat signal is suppressed, and contrast between normal and pathologic tissue is increased because of the synergistic effects of prolonged T1 and T2.

Head and Neck

The impact of MR on head and neck imaging was evident: 22 of the 23 papers presented on imaging of this area dealt with some application of MR. Several important papers focused on imaging of the temporomandibular joint (TMJ). A comparison of two-compartment TMJ arthrography and spin-echo MR showed that arthrography was superior in the detection of capsular effusions and perforation of the meniscus. On the other hand, MR was better for detecting intrinsic degeneration of menisci and surrounding soft tissue (Schellhas) (Fig. 12). MR was recommended as the procedure of choice for diagnosis of uncomplicated internal derangements of the TMJ; arthrography should be reserved for suspected effusion or perforation.

Technical improvements in MR imaging of the TMJ included the use of bilaterally positioned 3-in. (7.6-cm) surface coils connected to a combining device, allowing simultaneous bilateral TMJ imaging (Pressman). Because the time required for examination is reduced by 50%, conventional T1-weighted imaging can be used, thereby improving resolution over partial-flip-angle techniques. Additionally, because the images of each side are obtained simultaneously, a series of progressive jaw-opening images allows direct comparison of the two sides and evaluation of the motion-related abnormalities.

Gd-DTPA may have a major impact in MR imaging of head and neck tumors (Crawford; Schiller). Tumor conspicuity (Fig. 13) and size assessment were improved with enhancement. Gd-DTPA also improved definition of the tumor-muscle interface when compared with nonenhanced T1-weighted images, and it is especially useful in detecting recurrent tumor in head and neck cancer treated with radiation.

A description of the normal nasal cycle as depicted on MR was presented (Sinreich). Volunteers were imaged repetitively with MR over a 24-hr period. A cyclical side-to-side variation in signal intensity of the nasal and ethmoid mucosa was described. These normal changes may be interpreted incorrectly as sinus disease, and therefore the use of topical vasoconstrictive nasal spray 20 min before an MR study of this area is recommended.

The absence of a central cleft between the seventh and eighth cranial nerves within the internal auditory canal was reported as unreliable in excluding intracanalicular disease (Manzione). Gd-DTPA was advocated for the diagnosis of lesions of the seventh and eighth nerves because it increased both lesion conspicuity and detection of disease extent.

A practical method for the radiographic evaluation of masses found by either CT or MR in the spaces of the deep face was presented in a special session, "Radiology of the

Normal and Diseased Suprahyoid Neck" (Harnsberger and Dillon). The radiographic challenge of evaluating lesions discovered in the suprahyoid neck results from the complex anatomy of the region and the lack of a rational approach to interpretation of the images of mass lesions. The anatomy of the suprahyoid neck is best simplified by dividing the area into well-delineated spaces on the basis of the three layers of deep cervical fascia (Fig. 14). The principal five deep facial spaces to consider are the parapharyngeal, pharyngeal mucosal, masticator, parotid, and carotid. The parapharyngeal space, although it only contains fat, is the key space because of its central location relative to the remaining four spaces.

The method Harnsberger and Dillon presented for evaluation of a mass lesion discovered in the suprahyoid neck centers on assigning the lesion to one of the spaces described. This is done by determining the epicenter of the mass and its impingement pattern on the peripharyngeal space (Fig. 15). For example, a mass with its epicenter posterior to the peripharyngeal space from posterior to anterior must be in the carotid space (Fig. 15). Once the space of origin is assigned to the mass, the unique differential diagnosis of the space is matched to the radiographic features of the mass lesion to create a limited set of potential pathologic diagnoses that may be encountered by the surgeon.

By understanding the spatial anatomy of the suprahyoid neck and applying this method to evaluation of masses in this area, the radiologist can provide detailed preoperative information about both the critical neurovascular structures and the probable pathologic entities that will be met at the time of surgery.

Harnsberger and Dillon concluded by noting that head and neck imaging is an integral part of neuroradiology practice, linked to that subspecialty by the cranial nerves and skull, which are often involved by pathologic processes of the brain and extracranial head and neck.

Interventional Neuroradiology

Many exciting papers in interventional neuroradiology were presented. New accesses to difficult lesions included transvenous approaches (Fig. 16) to dural fistulas (Halbach; Goto) and aneurysms of the vein of Galen (Quisling; Lylyk) and direct puncture of inaccessible feeders (Berenstein). Complementing these novel approaches was the development of new and improved embolic agents, including platinum wires (some with thrombogenic fibers); cryoprecipitate; N-butyl-cyanoacrylate; and embolic mixtures of polyvinyl alcohol, collagen, and absolute alcohol (Brothers; Fox; Dion; Luedke; Yang; Hilal). When compared with more traditional agents, these materials offer improved safety in their delivery and a more permanent occlusion. Some alarming histologic findings have been reported with the use of liquid adhesives; these will need further study.

Several papers dealt with the endovascular treatment of intracranial aneurysms, most of which had been treated unsuccessfully with surgical clipping (Moret; Higashida; Hilal; Strother; Deveikis). These small series showed both impressive results and sobering complications, underscoring the need for improved methodology and experience in the treatment of these dangerous lesions.

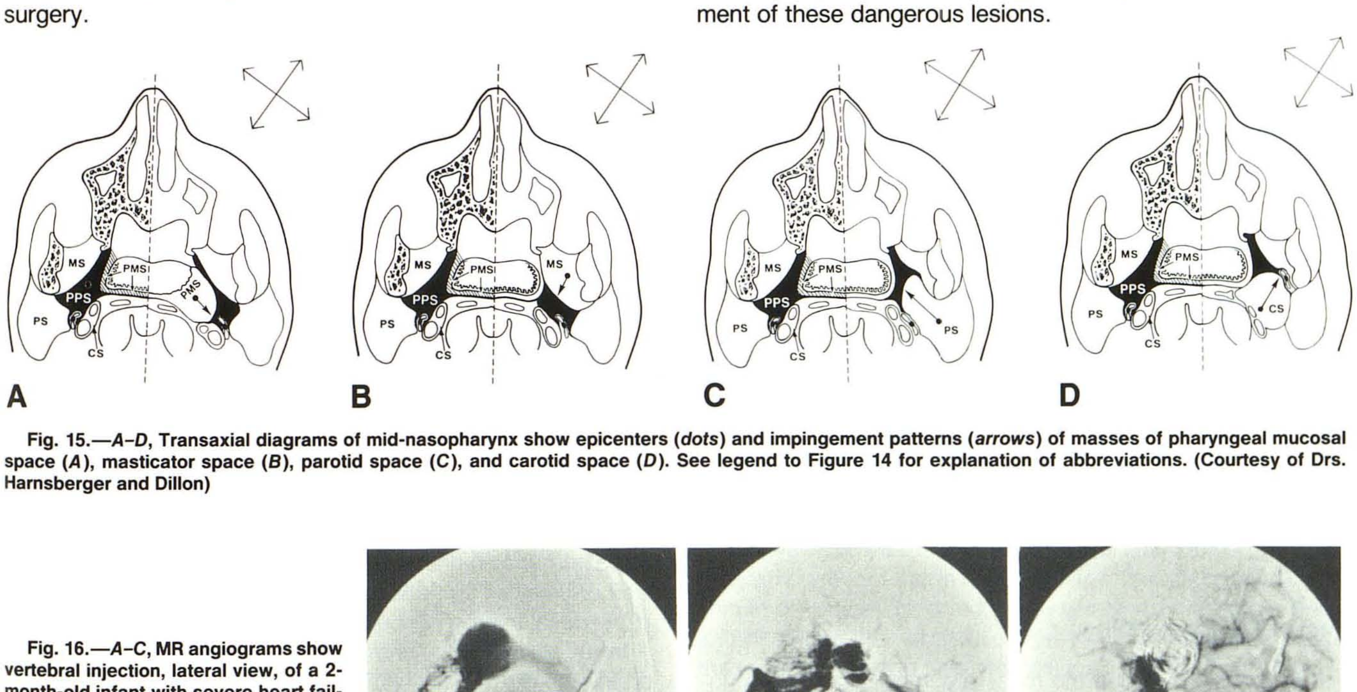

Fig. 15.—*A–D*, Transaxial diagrams of mid-nasopharynx show epicenters (*dots*) and impingement patterns (*arrows*) of masses of pharyngeal mucosal space (*A*), masticator space (*B*), parotid space (*C*), and carotid space (*D*). See legend to Figure 14 for explanation of abbreviations. (Courtesy of Drs. Harnsberger and Dillon)

Fig. 16.—*A–C*, MR angiograms show vertebral injection, lateral view, of a 2-month-old infant with severe heart failure and hydrocephalus associated with arteriovenous malformation with aneurysmal dilatation of vein of Galen before (*A*) and after partial (*B*) and complete (*C*) obliteration of fistula by transvenous embolization with multiple coils. (Courtesy of Drs. Higashida and Halbach)

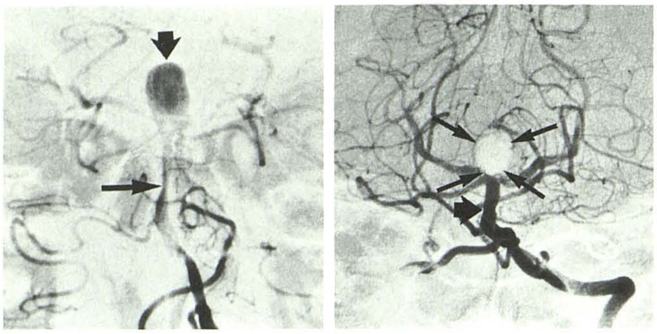

A B

Fig. 17.—*A*, Angiogram before treatment shows basilar tip aneurysm (*short arrow*) that has undergone hemorrhage with associated asymptomatic vasospasm (*long arrow*) in midbasilar artery. Zone of narrowing was dilated, and a balloon placed into aneurysm.

***B*, Follow-up angiogram shows complete obliteration of aneurysm (*long arrows*) and a normal caliber of mid-basilar artery (*short arrow*). (Courtesy of Drs. Higashida and Halbach)**

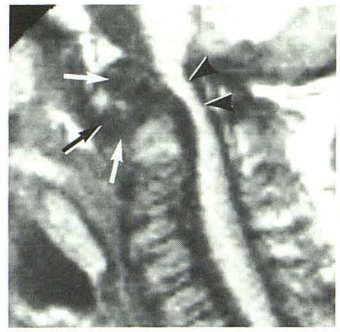

18

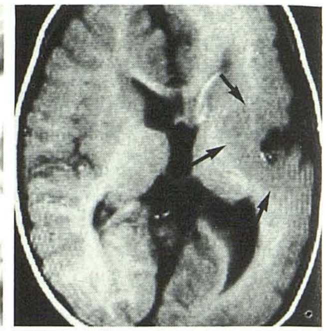

19

Fig. 18.—Sagittal T1-weighted MR image in a 20-year-old patient with type IV mucopolysaccharidosis (Morquio syndrome) shows dysplastic odontoid (*arrows*) with myelopathy caused by chronic C1–C2 subluxation. Note narrowed canal with deformed, impressed spinal cord (*arrowheads*). Vertebral bodies are flattened, ovoid in configuration, and poorly differentiated from intervertebral disks. (Courtesy of Dr. Sherman)

Fig. 19.—Axial T1-weighted MR image shows markedly abnormal left hemisphere with thickened cortical gray matter (*arrows*). Cerebral surface resembles pachygyria. Polymicrogyria was found at autopsy. (Courtesy of Dr. Byrd)

A series was presented on transluminal balloon occlusion of posterior circulation aneurysms (Fig. 17), and another paper discussed the results of angioplasty and treatment of symptomatic vasospasm by using balloon techniques (Higashida). A new double-lumen catheter was introduced that allows complete solidification of the balloon's contents within an aneurysm, thus preventing delayed recanalization, which could be disastrous when the parent artery is preserved. This design will allow the endovascular treatment of extremely small symptomatic aneurysms previously untreatable by endovascular techniques. In a special lecture, Charles Drake discussed the evolution in treatment of difficult cerebral aneurysms, including his view of the role of endovascular techniques (see section on President's Honorary Lecture).

The papers on interventional neuroradiology were not confined to vascular diseases. An invited lecture on percutaneous diskectomy described impressive results in a large symptomatic population when this new treatment was used (Onik). Of patients thus treated, 72% return to work within 2 weeks vs 6% of those treated by standard laminectomy. Onik predicted that cost-effectiveness and low morbidity should make this procedure even more commonplace. Another paper that presented the results of direct percutaneous biopsy of lesions causing complete myelographic blocks showed high diagnostic yields with low morbidity (Sutherland).

Pediatric Neuroradiology

MR imaging provided the most spectacular new contributions in the area of pediatric neuroradiology. Use of MR in children with myelodysplasia disclosed anatomic CNS information not previously available by noninvasive techniques (Boyer). Another application of MR was the evaluation of the craniovertebral junction in skeletal dysplasias (Fig. 18); flexion and extension sequences were deemed necessary for complete evaluation (Sherman). Some insight into the embryologic mechanisms that become deranged in dysraphism, teratoma, and caudal regression syndromes was provided by a paper that discussed spinal limbs (Naidich). Four patients with diastematomyelia and/or spinal lipoma had additional, occasionally functional, limbs arising from the midline back at sites from the cervical to the lumbar region. These extra limbs represent one end of a broad spectrum of anomalies associated with dysraphic twinning and caudal regression syndrome. A review of lumbar dermal sinuses found that they were midline in 80% and unilateral and paramedian in 30%, with 60% entering the spinal canal (Naidich). Thirty percent end in single or multiple (epi) dermoid tumors, and 20% are associated with postinfectious obliterative arachnoiditis.

MR findings simulating pachygyria are often due to polymicrogyria (Fig. 19) (Byrd). Pachygyria is seen most commonly with lissencephaly, as an isolated form, or in combination with dysmorphic facial syndromes (especially with a variant form of Miller-Dieker syndrome). Polymicrogyria cannot be diagnosed radiographically but can only be confirmed microscopically.

Multiple sclerosis in the pediatric age group accounts for 0.5–1.0% of all cases of this disease. Differences between adolescent multiple sclerosis and its adult counterpart included even more striking female prevalence, more severe disease, increased occurrence of posterior fossa disease, lack of atrophy, and absence of abnormal deposition of iron in the basal ganglia (Osborn).

In the diagnosis of primary CNS neuroblastoma, CT was preferable to MR (Davis). In a series of 11 patients with proved disease, five had typical large supratentorial masses, five had cysts, three had calcifications, and one had a spontaneous hemorrhage. Mass effect with little associated edema was characteristic. Atlantoaxial subluxation is more common in children and is another instance in which CT was described as the examination of choice (Port).

Extracorporeal membrane oxygenation (ECMO) provides temporary, mechanical cardiorespiratory support to full-term infants who have life-threatening but potentially reversible pulmonary or cardiac disease. Sonography provides a rapid safe method to detect a spectrum of intracranial complications of ECMO. Abnormalities recognized included focal parenchymal areas of altered echogenicity, which most likely were due to hematomas or to hemorrhagic or ischemic infarcts. Ischemic infarcts and nonhemorrhagic infarcts had identical sonographic appearances (Eelkema).

Special Features

President's Honorary Lecture

Charles Drake, Professor of Neurosurgery at the University of Western Ontario, gave the first annual ASNR President's Honorary Lecture. The lecture was dedicated to Juan M. Taveras, founding member and first president of the Society and editor-in-chief of the *American Journal of Neuroradiology*. Dr. Taveras was cited as "noted author, teacher, and investigator; eloquent spokesman for neuroradiology."

Dr. Drake spoke on the evolving management of intracranial aneurysms (i.e., current state of the surgical art that must be the benchmark for endovascular treatment). On the basis of his surgical experience with more than 3000 patients with intracranial aneurysms, Dr. Drake delineated the treatment of difficult giant aneurysms (600) and posterior or vertebrobasilar aneurysms (1500 patients). Careful preservation of vital perforating branches from the distal basilar and proximal posterior cerebral arteries, the use of temporary clips, and the development of finely crafted fenestrated surgical clips have significantly improved the outcome of these cases. Vasospasm with its attendant ischemic complications remains a problem; the return to early surgery with improved surgical results means more patients survive to develop vasospasm, though the prevalence of rebleeding is less.

Advances in catheter and balloon technology have made endovascular approaches appealing, particularly in patients who have perforating vessels arising from the neck, vessels with wide origins or impossible necks, or lack of collateral circulation that would permit proximal occlusion. Dr. Drake posed three issues for these innovative techniques: (1) technical problems, (2) control of their use, and (3) competitive morbidity rate compared with surgical approaches. A significant problem for any technique is incomplete occlusion, with residual aneurysm and the concomitant potential for regrowth. Approximately 5% of aneurysms clipped surgically had a minimal residual neck; he estimated that the recurrence risk is as high as 20% when a 1–2-mm neck remains. Custom-made or tailored balloons might eliminate this problem.

Dr. Drake appealed to interventional neuroradiologists to work as partners with neurosurgeons, citing the latter's expertise in overall care of these difficult patients with their complex management problems. He has abandoned embolization as the sole treatment of arteriovenous malformations, preferring to use it as a preoperative technique to reduce sump effect and lesion vascularity.

Finally, Dr. Drake stressed that the results of endovascular approaches must equal or better their surgical counterparts: for nongiant, unruptured anterior circulation aneurysms, no more than 1–2% morbidity; for recently ruptured lesions, 8–10%. Even endovascular treatment of basilar aneurysms is now associated with a less than 5% morbidity. For patients with giant aneurysms who were in good condition, the outcome was satisfactory in 89% on the anterior circulation, but only in 77% on the basilar system. Although many interventional neuroradiologists are admittedly treating only difficult cases rejected by neurosurgeons, these benchmarks must be kept in mind.

Special ASNR Symposium: Neuroradiology—The Future

Neil Chayet, an attorney who is well known for his nationally syndicated radio discussion of legal issues, spoke candidly, but hopefully, about the future of medicine. His premise was that we *can* make a difference, but we must make ourselves heard.

According to Mr. Chayet, government is no longer simply trying to reduce the expenditures for medical care, but now wants to control the mechanism itself. Unless the present trends are modified, physicians will be employees—and it is not clear who will write the paychecks.

We are fortunate to have wonderful technology available, but will they let us use it? Will we be paid appropriately for our expertise? Will we be sued if the results are not perfect? Government requires peer review but will not provide adequate safeguards against related lawsuits. Will cost-containment requirements of government and third-party payers be an adequate defense against malpractice suits arising as a result of our attempt to comply?—absolutely not.

Physicians must be aware of the recent legal decisions affecting malpractice actions. In a recent Massachusetts case, the court found that local standards of care no longer apply. Rather, it held that the applicable standards should be national. Issues about informed consent are now decided under the prudent-patient, not the prudent-doctor, doctrine.

The enemy is not the public. Rather it is the politicians, the press, and consumer groups, and that is a formidable alliance. How do physicians respond to this threat? We must become involved at all levels of organized medicine and in the political arena. Subspecialty organizations, Chayet thinks, have the capability to be influential well beyond their size, and they should wield that potential power.

Guidelines for the national standards of care, development of relative value scales and fee schedules, and expert-witness programs are just some arenas in which such organizations should be actively involved. If physicians are to restore pride and dignity to their profession, they must be willing to make the required effort to help themselves, Chayet stated.

Symposium on Issues in Neuroradiology

An innovative addition to the scientific program was a symposium on issues in neuroradiology that was organized and moderated by Michael Huckman and David O. Davis.

Discussants voiced opinions on future personnel needs in neuroradiology (Latchaw, Baker), future funding for graduate medical education (Binet), the neuroradiologist and the privately owned imaging center (Pressman, Chase), future directions in neuroradiology (Brant-Zawadzki, Taveras), new technologies and their impact on the subspecialty (Bryan, Di Chiro), the future of academic neuroradiology (Grossman, Hilal), ASNR and regional and technology-oriented societies (Quencer, Bergeron), and the training of nonneuroradiologists in invasive procedures (Hieshima, Newton). Several panelists emphasized the need for increased understanding and involvement in the basic neurosciences by neuroradiologists. Anne Osborn, ASNR President, 1988–1989, announced that the ASNR will be sponsoring a basic neuroscience course for clinical neuroradiologists to be held in the summer of 1989.

Technical Exhibits

Technical exhibits at ASNR meetings have grown steadily and impressively. Physicians attending the 1988 meeting could view rapidly and efficiently what industry leaders consider to be their major advances. The ASNR has become one of the two or three largest meetings at which new and sophisticated neuroimaging equipment, contrast media, and catheters and devices are displayed. The following were selected for comment by the Technical Exhibit Committee.

3D MR angiography was displayed by Siemens. With their postprocessing techniques, they were able to show that vessels could be disarticulated from surrounding anatomic tissue and displayed in an angiographic mode. This type of application has great potential to expand the capability of MR in the evaluation of cerebral vascular disease.

Comm View, an integrated system from AT & T and Philips also caught the eye. This combines a picture archiving and communication system with a radiology information system. The Comm View system can acquire, store, retrieve, and transmit patient information and anatomic images digitally.

General Electric showed their new Performance Plus option for updating their MR systems. Several components of the new systems—including a 192 × 256 acquisition matrix, fractional NEX imaging, and 3D fast-scan acquisitions—allow for considerable decrease in scanning time. A quadrature-drive head coil and a decoupled body coil also allow for improved image quality. Similarly, Picker announced upgraded software packages that will improve speed and efficiency and include FAST-II, MAST-II, and conjugate symmetry acquisition techniques.

In summary, the technical exhibits at the 1988 meeting were beneficial and informative. The growth of this particular component of our annual scientific meeting is a result of positive interaction between the ASNR leadership and administrative staff, industry, and the neuroradiologists themselves.

Books Received

Receipt of books is acknowledged as a courtesy to the sender. Books considered to be of sufficient interest will be reviewed as space permits.

Neurocardiology. Edited by Henri E. Kulbertus and Georges Franck. Mount Kisco, NY: Futura, 364 pp., 1988. $59.50

Vascular and Multi-Infarct Dementia. Edited by John Stirling Meyer, Helmut Lechner, John Marshall, and James F. Toole. Mount Kisco, NY: Futura, 276 pp., 1988. $39

Muscle Disease. Edited by Jack E. Riggs. (vol. 6 in Neurologic Clinics.) Philadelphia: Saunders, 648 pp., August 1988.

Pediatric Cerebrovascular Disorders. By E. S. Roach and Anthony R. Riela. Mount Kisco, NY: Futura, 257 pp., 1988. $45

Prostaglandin and Lipid Metabolism and Radiation Injury. Edited by Thomas L. Walden and Haywood N. Hughes. New York: Plenum, 420 pp., 1987. $72.50

Computed Tomography of the Pituitary Gland. By M. J. Hendriks. Assen/Maastricht: the Netherlands, 126 pp., 1988.

Introduction to Clinical Neuroscience, 2d ed. By John Walton. Philadelphia: Saunders, 282 pp., 1988. $22.95

Vascular Anatomy of the Spinal Cord. By Armin K. Thron. New York: Springer-Verlag, 114 pp., 1988. $59.50

Clinical Atlas of Auditory Evoked Potentials. Edited by Jeffrey H. Owen and Charles D. Donohoe. Philadelphia: Saunders, 119 pp., 1988. $44

Radiology of Facial Injury, 2d ed. By Kenneth D. Dolan, Charles G. Jacoby, and Wendy R. K. Smoker. New York: Macmillan, 103 pp., 1988. $49.95

Magnetic Resonance Imaging. Atlas of the Head, Neck, and Spine. By Catherine M. Mills, Jack de Groot, and Jonathan P. Posin. Philadelphia: Lea & Febiger, 295 pp., 1988. $98.50

Interventional Radiology. By Wilfrido R. Castaneda-Zuniga and S. Murthy Tadavarthy. Baltimore: Williams & Wilkins, 873 pp., 1988. $149.95

Soft Tissue Tumors, 2nd ed. By Franz M. Enzinger and Sharon W. Weiss. St. Louis: Mosby, 989 pp., 1988.

Imaging and Correlative Physicochemical Techniques. Edited by Alan A. Boulton, Glen B. Baker, and Donald P. J. Boisvert. (vol. 8 in Neuromethods.) Clifton, NJ: Humana Press, 460 pp., 1988. $69.50

Imaging of Vertebral Trauma. By Richard H. Daffner. Rockville, MD: Aspen, 165 pp., 1988.

Imaging of the Foot and Ankle. By D. M. Forrester, Morrie E. Kricun, and Roger Kerr. Rockville, MD: Aspen, 325 pp., 1988.

Brain Anatomy and Magnetic Resonance Imaging. Edited by A. Gouaze and G. Salamon. New York: Springer-Verlag, 189 pp., 1988. $89

Cross-Sectional Anatomy for Computed Tomography. By Michael L. Farkas. New York: Springer-Verlag, 84 pp., 1988. $35

National Council on Radiation Protection and Measurements Reports: No. 92: Public Radiation Exposure from Nuclear Power Generation in the United States; No. 94: Exposure of the Population in the United States and Canada from Natural Background Radiation; No. 95: Radiation Exposure of the U.S. Population from Consumer Products and Miscellaneous Sources. Bethesda, MD: National Council on Radiation Protection and Measurements, 1987.

Erratum

In the special section summarizing the 1988 ASNR meeting that appeared in the September/October 1988 issue of the Journal (Osborn AG, Pressman BD, Dillon WP, et al., Advances in Neuroimaging, *AJNR* **1988;**9:985–994), an error was made in reporting the findings of Dr. Schellhas. On page 990, under the heading "Head and Neck," line 7 should read "detection of capsular *adhesions*" (not "effusions"). The authors apologize for this error.